Available online at www.sciencedirect.com

SCIENCE DIRECT

Biochimica et Biophysica Acta 1743 (2005) 255–267

BIOCHIMICA ET BIOPHYSICA ACTA BBA

http://www.elsevier.com/locate/bba

The aldehyde acrolein induces apoptosis via activation of the mitochondrial pathway

André Tanel, Diana A. Averill-Bates*,[1]

Département de chimie et de biochimie, TOXEN, Université du Québec à Montréal CP 8888, Succursale Centre Ville, Montréal, Québec, Canada H3C 3P8

Received 7 June 2004; received in revised form 10 November 2004; accepted 15 November 2004
Available online 20 December 2004

Abstract

Acrolein is a highly reactive α,β-unsaturated aldehyde, which is a product of lipid peroxidation. It is an environmental pollutant that has been implicated in multiple respiratory diseases. Acrolein is produced by the enzymatic oxidative deamination of spermine by amine oxidase. Oxidation products of polyamines have been involved in the inhibition of cell proliferation, apoptosis, and the inhibition of DNA and protein synthesis. The present study investigates the mechanism of cell death induced by acrolein. Acrolein induced apoptosis through a decrease in mitochondrial membrane potential, the liberation of cytochrome *c*, the activation of initiator caspase-9, and the activation of the effector caspase-7. However, acrolein inhibited enzymatic activity of the effector caspase-3, although a cleavage of pro-caspase-3 occurred. The activation of caspases-9 and -7 was confirmed by the cleavage of their pro-enzyme form by acrolein. Apoptosis was inhibited by an inhibitor of caspase-9, but not by an inhibitor of caspase-3. The induction of apoptosis by acrolein was confirmed morphologically by the condensation of nuclear chromatin and by the cleavage of the inhibitor of caspase activated DNase (ICAD), which leads to the liberation of CAD that causes DNA fragmentation. These results demonstrate that acrolein causes apoptosis through the mitochondrial pathway.

Keywords: Acrolein; Apoptosis; Caspase; Mitochondria; Cell; Cytotoxicity

1. Introduction

Acrolein is a highly reactive α,β-unsaturated aldehyde, and humans are exposed to this compound in multiple situations [1]. Acrolein is one of the toxic products of endogenous lipid peroxidation (LPO) [2]. Acrolein is a major component of cigarette smoke and a constituent of automotive exhaust [3]. Industrially, acrolein is used as a herbicide as well as a starting material for acrylate polymers and in the production of acrylic acid [4]. Acrolein reacts with the cysteine, histidine, and lysine residues of proteins [5,6]. Acrolein protein adducts have been demonstrated in diabetic nephropathy [7], Alzheimer's disease [8,9], and atherosclerosis [10].

Apoptosis is a physiological cell death process which plays an important role during the development and maintenance of tissue homeostasis [11,12]. A balance between cell death and cell proliferation is required to maintain a cellular homeostatic state. Deviation from this cellular balance disrupts the normal state and can lead to human disease [13]. A family of cytosolic cysteine proteases, the caspases, stored in most cells as zymogens, plays an essential role in the execution of apoptosis. The

Abbreviations: AFC, amino trifluorocoumarin; AMC, amino methylcoumarin; BSA, bovine serum albumin; BSAO, bovine serum amine oxidase; CAD, caspase activated DNase; CHAPS, 3-[(3-cholamidopropyl)dimethylammonio]-2-hydroxy-1-propanesulfonic acid; CHO, Chinese hamster ovary; Fas, fibroblast-associated; FBS, fetal bovine serum; FCCP, *P*-trifluoromethoxy-phenyl-hydrazone; ICAD, inhibitor of caspase activated DNase; MEM, minimum essential medium; MOPS, 3-(*N*-morpholino)-propane sulfonic acid; PARP, polyADP-ribose polymerase; PBS, phosphate-buffered saline; PMSF, phenylmethylsulfonyl fluoride; PTP, permeability transition pore; PVDF, polyvinylidene difluoride; SDS-PAGE, sodium dodecyl sulfate-polyacrylamide gel electrophoresis; SE, standard error

* Corresponding author. Tel.: +1 514 987 3000x4811; fax: +1 514 987 4054.
E-mail address: averill.diana@uqam.ca (D.A. Averill-Bates).
[1] Formerly Dr. Diana A. Bates.

0167-4889/$ - see front matter © 2004 Elsevier B.V. All rights reserved.
doi:10.1016/j.bbamcr.2004.11.007

caspases are divided into apical (-2, -8, -9, and -10) and executioner subsets (-3, -6, and -7) [14]. The zymogen of caspase-9 is activated via a post-mitochondrial route [15].

The mitochondrial pathway is triggered by growth factor deprivation, ionizing radiation, and some anticancer drugs such as cyclophosphamide and etoposide [16]. Cytochrome *c* is released from the mitochondria into the cytosol, where it interacts with dATP and apoptosis protease activating factor (Apaf1) and pro-caspase-9 in the apoptosome complex in the cytosol. This leads to the conversion of pro-caspase-9 to active caspase-9 [17]. Anti-apoptotic (Bcl-2) and pro-apoptotic (Bax) members of the Bcl-2 family are thought to control apoptosis by modulating cytochrome *c* release from the mitochondria [18]. Once activated, caspase-9 activates effector caspases such as caspases-3, -6, and -7 [14]. Effector caspases then cleave specific cytoplasmic, cytoskeletal, and nuclear protein substrates such as polyADP-ribose polymerase (PARP), lamins, and inhibitor of caspase activated DNase (ICAD). The cell then exhibits the characteristic morphological features of apoptosis such as chromatin condensation, cell blebbing, and formation of apoptotic bodies [19].

Acrolein has been shown to induce apoptosis in cell types such as human alveolar macrophages [20], human keratinocytes [21], and human bronchial epithelial cells HBE1 [22]. In contrast, acrolein inhibited neutrophil apoptosis [23] and induced oncosis/necrosis rather than apoptosis in murine proB lymphocytes [24]. Thus, acrolein-induced apoptosis appears to be cell type dependent. Most of these studies confirmed the induction of apoptosis by means of endpoints occurring later in the apoptotic cascade such as DNA fragmentation, without determining the mechanisms occurring upstream of these events.

Acrolein is a metabolic product of cyclophosphamide [25] and could be involved in its anticancer action. It is also a product of the oxidation of polyamines by amine oxidases along with hydrogen peroxide [26]. Our previous studies suggest that amine oxidase could prove to be useful in cancer treatment [27]. Targeting polyamines has emerged as a promising therapeutic strategy since they play an important role in the development and maintenance of neoplastic growth [28]. Moreover, rapidly growing tissues such as tumors have elevated levels of polyamines [29]. To take advantage of this differential effect between normal and tumor cells, toxic products such as H_2O_2 and aldehydes could be generated in situ by amine oxidases for the selective killing of tumor cells [30]. However, the molecular mechanisms involved in acrolein-induced apoptosis in cancer cells are not understood. This study investigates the ability of acrolein to activate apoptosis via the mitochondrial pathway in proliferating Chinese hamster ovary (CHO) cells, which are known to induce tumors.

2. Materials and methods

2.1. Cell culture

CHO cells (AuxBl) [31] were grown in monolayer in minimum essential medium-Alpha (α-MEM) (Gibco Canada, Burlington, ON, Canada) plus 10% fetal bovine serum (FBS) (Gibco Canada) and 1% penicillin (50 units/mL)-streptomycin (50 μg/mL) (Flow Laboratories, Mississauga, ON, Canada) in tissue culture flasks (Starstedt, St Laurent, QC, Canada), in a humidified atmosphere of 5% CO_2 in a water jacketed incubator at 37 °C [32]. The cells were grown to near confluence and were then incubated for 24 h with fresh culture medium. Confluent cells were then harvested using citrated phosphate-buffered saline (0.14 M NaCl, 0.01 M sodium phosphate, 0.015 M sodium citrate), washed by centrifugation (1000×*g*, 3 min), and resuspended in α-MEM for experimental studies.

2.2. Clonogenic cytotoxicity assay

Cytotoxicity was evaluated as the ability of cells to proliferate to form macroscopic colonies after a toxic insult with acrolein, using a clonogenic cell survival assay. CHO cells (10^5/mL) were incubated with acrolein (Aldrich Chemical Co, Milwaukee, WI), in a final volume of 1.0 mL, in α-MEM containing 10% FBS for 1 h at 37 °C. The cells were then washed three times by centrifugation (1000×*g*, 2 min) to stop the incubation [32]. The cells were resuspended and diluted to the appropriate concentration with α-MEM plus FBS and plated in tissue culture dishes (60×15 mm), which were incubated at 37 °C in an atmosphere of 5% CO_2 for 8 days. The dishes were then washed with PBS, fixed with 95% ethanol, and stained with methylene blue before counting macroscopic colonies (>50 cells). Cytotoxicity was expressed as the mean number of colonies obtained relative to the mean number of colonies obtained in the control. Two hundred cells were seeded in the control plates, but where there was a loss of cell survival, cells were plated at several different densities to ensure that countable colonies would be obtained, and the results were corrected accordingly. We have previously demonstrated that, in this system, there is linearity between the number of cells plated and colonies formed over the range of 10 to 10^4 [32].

2.3. Morphological analysis of apoptosis

To visualize nuclear morphology and chromatin condensation by fluorescence microscopy [33], cells were seeded and cultured to near confluence in tissue culture dishes containing 5 ml of α-MEM and 10% FBS. Cells were incubated with acrolein for 4 h or 24 h. Dishes were washed twice with PBS, and Hoechst (33258) (0.06 mg/ml) was added for 15 min at 37 °C to stain apoptotic cells. The

dishes were washed with PBS, and propidium iodide (50 μg/ml) was added to stain the necrotic cells. Observations were made by fluorescence microscopy (Carl Zeiss Ltd, Montreal, QC), and photographs were taken by digital camera (camera 3CCD, Sony DXC-950P, Empix Imaging Inc, Mississauga, ON). Images were analysed by Northern Eclipse software. Cells were classified using the following criteria: (a) live cells (normal nuclei, pale blue chromatin with organized structure); (b) membrane-intact apoptotic cells (bright blue condensed or fragmented chromatin); (c) necrotic cells (red, enlarged nuclei with smooth normal structure [33]). The fractions of apoptotic and necrotic cells were determined relative to the total cells (obtained using bright field illumination). A minimum of 200 cells were counted per dish.

2.4. Caspase inhibitors

The treatment of cells with the inhibitors of caspases was performed on confluent cells in monolayer. The specific inhibitors used were the following: Caspase-3 Inhibitor V, Z-DQMD-FMK; Caspase-9 Inhibitor I, Z-LEHD-FMK; and the general Caspase Inhibitor I, Z-VAD-FMK (Calbiochem, La Jolla, CA). The cells were exposed to 10 or 20 μM concentrations of inhibitors and to various concentrations of acrolein for 4 h. Cells were analysed for apoptosis by fluorescence microscopy using Hoescht staining.

2.5. Determination of caspase activity by fluorescence spectroscopy

Freshly harvested CHO cells (0.5×10^6) were resuspended in α-MEM and incubated with acrolein in a final volume of 1.0 mL at 37 °C. After the appropriate time, the cells were washed three times with cold PBS by centrifugation ($1000\times g$, 3 min) to stop the incubation. The cells were resuspended in 50 μl of PBS, and 25 μl was deposited into 96-well plates and lysed by freezing at −20 °C for 20 min. Fifty microliters of reaction buffer (20 mM piperazine-*N*,*N*′-bis(2-ethanesulfonic acid) (PIPES), 100 mM NaCl, 10 mM dithiothreitol, 1 mM EDTA, and 0.1% 3-[(3-cholamidopropyl)dimethylammonio]-2-hydroxy-1-propanesulfonic acid (CHAPS), 10% sucrose, pH 7.2) was added and stabilized at 37 °C [34]. The kinetic reaction was started after the addition of 25 μl of the appropriate caspase substrate at 37 °C, using a Spectra Max spectrofluorimeter (Spectra Max Gemini, Molecular Devices, Sunnyvale, CA).

Caspase-3 activity was measured by the cleavage of the fluorogenic substrate *N*-acetyl-Asp-Glu-Val-Asp-amino-4-methylcoumarin (Calbiochem, La Jolla, CA) to produce amino methylcoumarin (AMC) with λ_{max} excitation at 380 nm and λ_{max} emission at 460 nm. Caspase-7 activity was measured by the cleavage of the fluorogenic substrate I MCA-VDQVDGWK(DNP)-NH_2 with λ_{max} excitation at 325 nm and λ_{max} emission at 395 nm. Caspase-9 activity was measured by cleavage of the substrate Ac-LEHD-AFC to produce AFC with λ_{max} excitation at 415 nm and λ_{max} emission at 490 nm.

2.6. Flow cytometry analysis of mitochondrial membrane potential

To measure $\Delta\psi m$, the fluorescent probe rhodamine 123 was used. Freshly harvested CHO cells (10^6) were resuspended in α-MEM and incubated with acrolein, or the positive control *p*-trifluoromethoxy-phenyl-hydrazone (FCCP), in a final volume of 1.0 mL at 37 °C. After 1 h of incubation, the cells were washed three times with cold PBS by centrifugation ($1000\times g$, 3 min) to stop the incubation. The cells were resuspended with PBS and then incubated with the fluorescent probe (800 ng/ml) for 5 min. Samples were washed and stored in the dark at 4 °C until the time of analysis (usually within 5 min). Propidium iodide (PI) was added to cell suspensions stained with rhodamine 123 to identify dead cells. Cells were analysed with a FACScan flow cytometer equipped with an argon laser emitting at 488 nm (Becton Dickinson, Oxford, UK). Data was acquired and analysed using Lysis II software (Becton Dickinson). The mean fluorescence intensity of 20,000 cells was calculated for each sample and corrected for autofluorescence obtained from the samples of unlabeled cells. The analyser threshold was adjusted on the forward scatter (FSC) channel to exclude noise and subcellular debris. Photomultiplier settings were adjusted to detect rhodamine 123 fluorescence on the FL1 detector and PI fluorescence on the FL2 detector. In each case, the photomultiplier voltage was set so that the signal peak from non-stained cells (mostly due to autofluorescence) fell within the first decade of the logarithmic amplifier. Light scatter parameters were used to establish size gates which detect apoptotic cells, thus excluding dead cells [35]. Populations of dead cells highly fluoresce in FL2 because they incorporate PI, thus 2 populations of cells appear on the computer screen. For each sample, only the live cells are selected, and their mean fluorescence in FL1 is analysed. Apoptotic cells, which undergo a decrease in mitochondrial membrane potential, incorporate less of the rhodamine 123 dye, therefore emitting less fluorescence on the FL1 detector.

2.7. Subcellular fractionation and immunodetection of cytochrome c, caspases, and ICAD

Following treatment with acrolein, cells were washed in buffer A (100 mM sucrose, 1 mM EGTA, 20 mM MOPS, pH 7.4) and resuspended in buffer B [buffer A plus 5% Percoll, 0.01% digitonin, and a cocktail of protease inhibitors: 10 μM aprotinin, 10 μM pepstatin A, 10 μM leupeptin, 25 μM calpain inhibitor I, and 1 mM phenylmethylsulfonyl fluoride (PMSF)]. After a 30-min

incubation on ice, lysates were homogenised using a hand potter (Kontes glass CO, Duall 22, Fisher, QC, Canada). Unbroken cells and nuclei were pelleted by centrifugation at 2500×*g* for 10 min. The supernatant was centrifuged further at 100 000×*g* for 1 h. The resultant supernatant was designated as the cytosolic fraction, which was used for the detection of cytochrome *c*. For the immunodetection of caspases and ICAD, whole cell lysates were used.

SDS-polyacrylamide gel electrophoresis (SDS-PAGE) of the cellular proteins was carried out according to Laemmli [36]. Proteins (30 μg) were quantified according to Bradford [37] and then solubilised in Laemmli sample buffer. The samples were boiled for 5 min at 100 °C and loaded onto a 15% acrylamide gel. Electrophoresis was carried out at a constant voltage of 125 V. Cellular proteins were transferred electrophoretically to a polyvinylidene difluoride (PVDF) membrane using a MilliBlot Graphite Electroblotter I apparatus (Milli-pore, Bedford, MA). The transfer buffer contained 96 mM glycine, 10 mM Tris, and 10% methanol. The transfer was carried out for 1.5 h at a constant amperage of 80 mA/gel. Hydrophobic or non-specific sites were blocked overnight at 4 °C with 5% powdered skim milk in Tris-buffered saline (50 mM Tris and 150 mM NaCl) containing 0.1% Tween 20 (TBS-T). Membranes were washed four times for 15 min in TBS-T. The blots were probed with the primary antibody anti-cytochrome *c* (BD Biosciences Canada, Mississauga, ON), anti-caspase-3, anti-caspase-9, anti-ICAD, anti-tubulin (Santa Cruz Biotechnology, Santa Cruz, CA), and anti-caspase-7 (Cell Signaling Technology, Beverly, MA) in TBS-T, 1% bovine serum albumin (BSA) for 1 h at room temperature. Membranes were washed four times for 15 min and incubated for 1 h at room temperature with peroxidase-conjugated secondary antibody (1:1000) in TBS-T containing 5% milk powder. Secondary antibodies consisted of horseradish peroxidase (HRP)-conjugated goat anti-mouse, anti-rabbit, and anti-goat IgG (Biosource, Camarillo, CA). PVDF membranes were washed four times for 15 min, and cytochrome *c*, caspases, and ICAD were detected using the ECL plus chemiluminescence kit (PerkinElmer, Boston, MA). For verification of equivalence in protein loading, the blot was probed with the anti-tubulin antibody and by coloration of the membrane using Coomassie blue. Protein expression was quantified using a scanning laser densitometer, relative to β-tubulin (Molecular Dynamics, Sunnyvale, CA).

2.8. Statistical analysis

Statistical differences between the control and treated groups for cell survival and ICAD cleavage were determined by a two-tailed unpaired Student's *t* test. Statistical comparisons for the glutathione assay were made with one-way ANOVA, which measures the linear contrast of means. An adjustment was made to limit the family-wise error rate (FWE) to 5% by calculating an adjusted *P*-value, which is a simulated based *P*-value obtained from the multivariate *t* distribution (number of simulations=1 000 000) [38]. Two-way ANOVA with a *P*-adjusted value obtained using the Bonferroni–Holm method (a stepwise method) was used to compare cells treated with acrolein versus the control, using the Hoescht test. Data for caspase activity and caspase cleavage were analysed for significant differences using a one-way ANOVA with a Bonferroni–Holm post-test correction for multiple comparisons. For experiments involving caspase inhibitors, adjusted *P*-values were obtained using one-way ANOVA, followed by the Dunnett test.

Values are expressed as means±S.E. Differences were considered statistically significant at $P<0.05$.

3. Results

We established the concentrations of acrolein which were able to induce cytotoxicity in CHO cells (Fig. 1). Cytotoxicity was induced at concentrations of 50 fmol/cell of acrolein and higher. A concentration of about 180 to 190 fmol/cell (18–19 μM) was sufficient to decrease the fraction of surviving cells to 10%. Above 200 fmol/cell, there was a marked decline in cell survival to 5 logarithms of cell killing at 350 fmol/cell. It should be noted that the acrolein concentration was expressed as fmol/cell because the cell density was different for certain tests [39].

Subsequently, we investigated the type of cell death (i.e., apoptosis or necrosis) induced by acrolein in proliferating CHO cells. Morphological analysis demon-

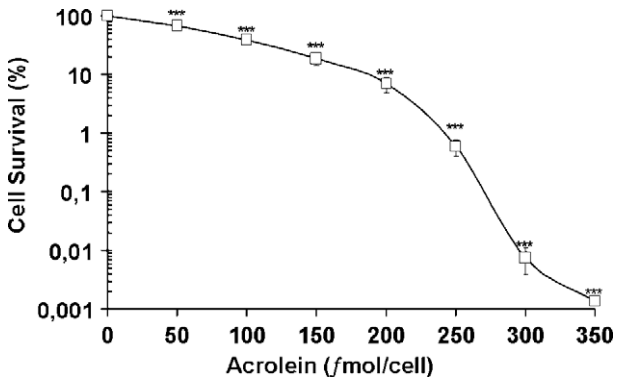

Fig. 1. Induction of cytotoxicity by acrolein. Cytotoxicity was assessed by a clonogenic cell survival assay. CHO cells (10^5/ml) were exposed to acrolein (50 to 350 fmol/cell) for 1 h at 37 °C in 1 ml of α-MEM containing 10% FBS. Acrolein was then removed, and cells were incubated in culture dishes for 8 days to allow the formation of macroscopic colonies (see Methods). The control value represents 10^5 cells and this was normalized to represent 100% cell survival. There is a significant difference between cells treated with acrolein, relative to untreated controls, $P<0.001$ (***). Data represent means and S.E. from four independent experiments performed with multiple estimations per point. When not shown, error bars lie within the symbols.

strates that acrolein induces both apoptosis and necrosis in cells (Fig. 2). Apoptosis is characterized by the early and prominent condensation of nuclear chromatin [33]. Apoptosis induced by acrolein was revealed by the condensation of chromatin with the fluorescent probe Hoescht (blue–green), whereas necrosis was revealed by the fluorescent probe PI (red). Acrolein (50 fmol/cell, 4 h) (Fig. 2C) induced apoptosis and necrosis in 21% and 4% of cells, respectively (Fig. 2E, F). A higher concentration of acrolein (100 fmol/cell, 4 h) (Fig. 2D) switched the mode of cell death from apoptosis (9%) to necrosis (20%) (Fig. 2E, F). It should be pointed out that the induction of apoptosis occurred at lower concentrations of acrolein (≥30 fmol/cell, 4 h) (Fig. 2B, E), relative to the induction of necrosis (≥50 fmol/cell, 4 h) (Fig. 2C, F). Very few dead cells were seen in the untreated controls (Fig. 2A). When cells were exposed to acrolein for 24 h, higher levels of toxicity occurred by apoptosis and necrosis (Fig. 2E, F). Maximum levels of apoptosis were induced by 30 and 50 fmol/cell of acrolein, whereas 100 fmol/cell of acrolein caused essentially only necrosis.

The subsequent step was to determine whether acrolein could induce apoptosis via the activation of the mitochondrial pathway. The ability of acrolein to alter mitochondrial membrane potential and to induce the liberation of cytochrome *c* from the mitochondria to the cytosol was determined. Exposure of cells to acrolein (10 to 30 fmol/cell) for 1 h led to a decrease in rhodamine 123 fluorescence in the FL1 channel, relative to the untreated control cells (Fig. 3A, B). This represented a decrease in mitochondrial membrane potential by 25% in the presence of 30 fmol/cell of acrolein, relative to controls (Fig. 3B). The magnitude of the decrease was similar to that induced by FCCP (5 μM), which was used as a positive control

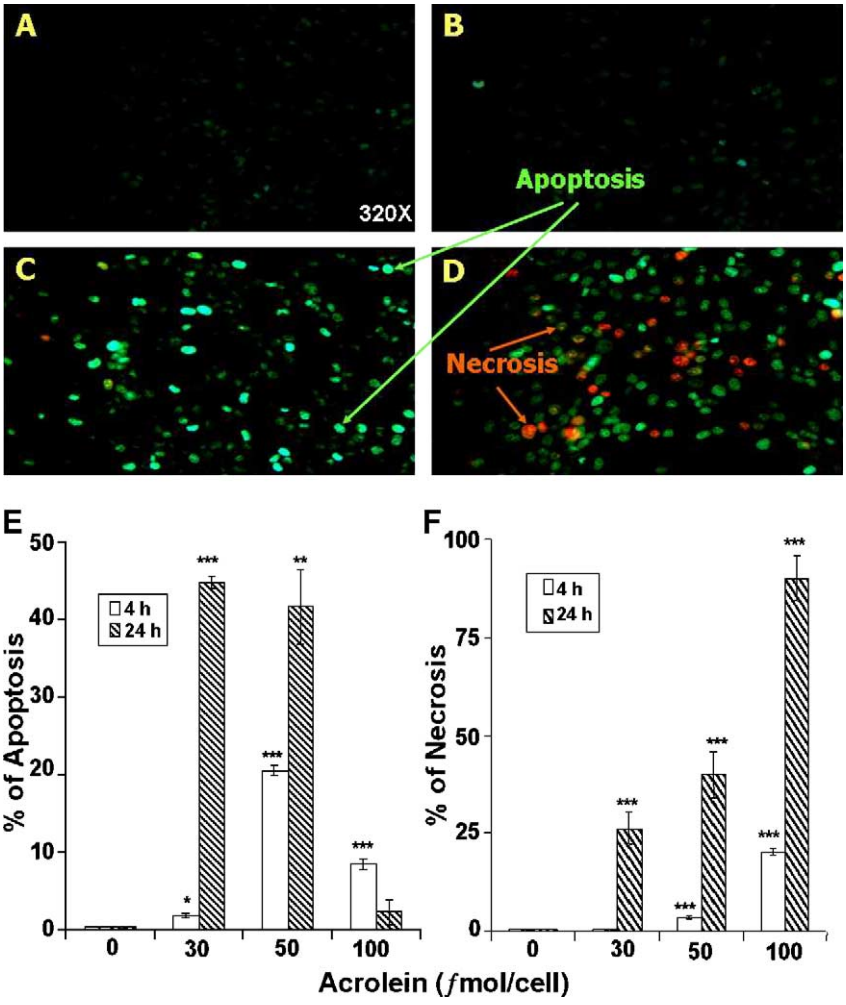

Fig. 2. Morphological analysis of apoptosis and necrosis in cells following exposure to acrolein. Cells (0.3×10^6) were seeded and cultured for 2 days to near confluence in tissue culture dishes containing α-MEM and 10% FBS at 37 °C. Cells were incubated with different concentrations of acrolein: (A) 0, (B) 30, (C) 50 and (D) 100 fmol/cell, for 4 h. Cells were stained with Hoechst and PI and visualised by fluorescence microscopy (magnification 320×). The fractions of (E) apoptotic and (F) necrotic cells following treatment with acrolein for 4 h and 24 h are given relative to total cells. A minimum of 600 cells were counted per dish. Data represent means and S.E. from four or five independent experiments performed with multiple estimations per point. $P<0.05$ (*), $P<0.01$ (**), or $P<0.001$ (***) indicates a statistically significant difference between treatment with acrolein and the control.

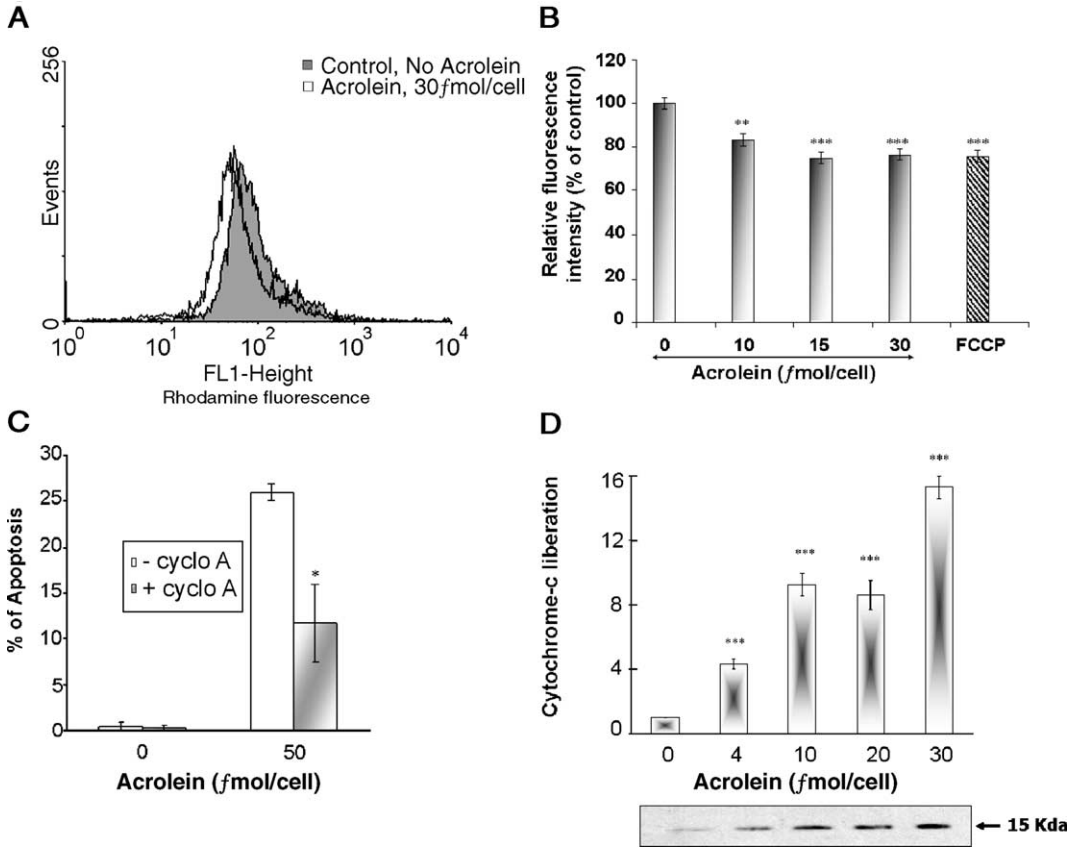

Fig. 3. Acrolein induces depolarization of the mitochondrial membrane and liberation of cytochrome *c*. (A) CHO cells (10^6/ml) were incubated with acrolein (30 fmol/cell) (white) for 1 h at 37 °C in α-MEM and 10% FBS, relative to untreated control cells (grey), and then analysed by flow cytometry for rhodamine 123 (800 ng/ml) fluorescence in channel FL1. (B) Data represent means and S.E. of relative fluorescence intensity of rhodamine from seven independent experiments. $P<0.01$ (**) or $P<0.001$ (***) indicates a statistically significant difference between treatment with acrolein or FCCP and the control. The absolute data value for the untreated control cells from 7 experiments was 39±3 (mean±S.E.) relative fluorescence units. The control value was designated as 100%, and other data values in FCCP- and acrolein-treated cells were normalized to this point. (C) Cells were incubated with acrolein, with or without 5 μM cyclosporine A, for 4 h, and then stained with Hoechst and PI. A minimum of 600 cells were counted per dish. Data represent means and S.E. from four independent experiments performed with multiple estimations per point. $P<0.05$ (*) indicates a statistically significant difference between treatment with acrolein with or without cyclosporine A. (D) Cells (10^6/ml) were incubated with acrolein (4 to 30 fmol/cell) for 1 h in α-MEM containing 10% FBS. The immunodetection of cytochrome *c* was carried out by SDS-PAGE, using β-tubulin as a loading control (not shown). A representative gel is shown from four independent experiments. The expression of cytochrome *c* was relative to the untreated control, designated as 1. Data represent means and S.E. for gels from four independent experiments. $P<0.001$(***) indicates a statistically significant difference between acrolein treatment and control.

for membrane depolarisation (Fig 3B). The mitochondrial permeability transition pore (PTP) complex is considered to play an important role in the release of pro-apoptotic proteins such as cytochrome *c*. The opening of the PTP can be inhibited by compounds such as cyclosporine A [40]. Indeed, cyclosporine A partially inhibited apoptosis induced by acrolein (Fig. 3C), further confirming the role of membrane depolarisation in acrolein-induced apoptosis. Acrolein (4 to 30 fmol/cell) caused the liberation of cytochrome *c* after 1 h (Fig. 3D). Exposure to acrolein (1 to 50 fmol/cell) for 1 h caused the activation of caspase-9, which is the initiator caspase of the mitochondrial pathway (Fig. 4A). However, after 2 h, there was no activation of caspase-9, but instead, an inhibition of the enzyme. In fact, caspase-9 activity was lower than the control level for concentrations between 20 and 150 fmol/cell, although this was only significant at the highest dose. We found that acrolein cleaved procaspase-9 as a function of increasing concentration from 2 to 50 fmol/cell after a 1-h incubation (Fig. 4B, C). This was apparent as a decrease in the intensity of bands (Fig. 4B) for the pro-enzyme form of caspase-9 (Fig. 4C). There was a corresponding increase in the quantity of cleavage fragment of 35 kDa for caspase-9 (Fig. 4B, D) with increasing acrolein concentration.

We subsequently determined the ability of acrolein to activate effector caspases. However, the enzymatic activity of the major downstream effector caspase-3 was inhibited by low concentrations of acrolein (5 to 20 fmol/cell) (Fig. 5A). Caspase-3 activity was rapidly inhibited after exposure to acrolein for only 5 min (Fig. 5A). Indeed, the exposure of cells to 20 fmol/cell of acrolein for 1 h

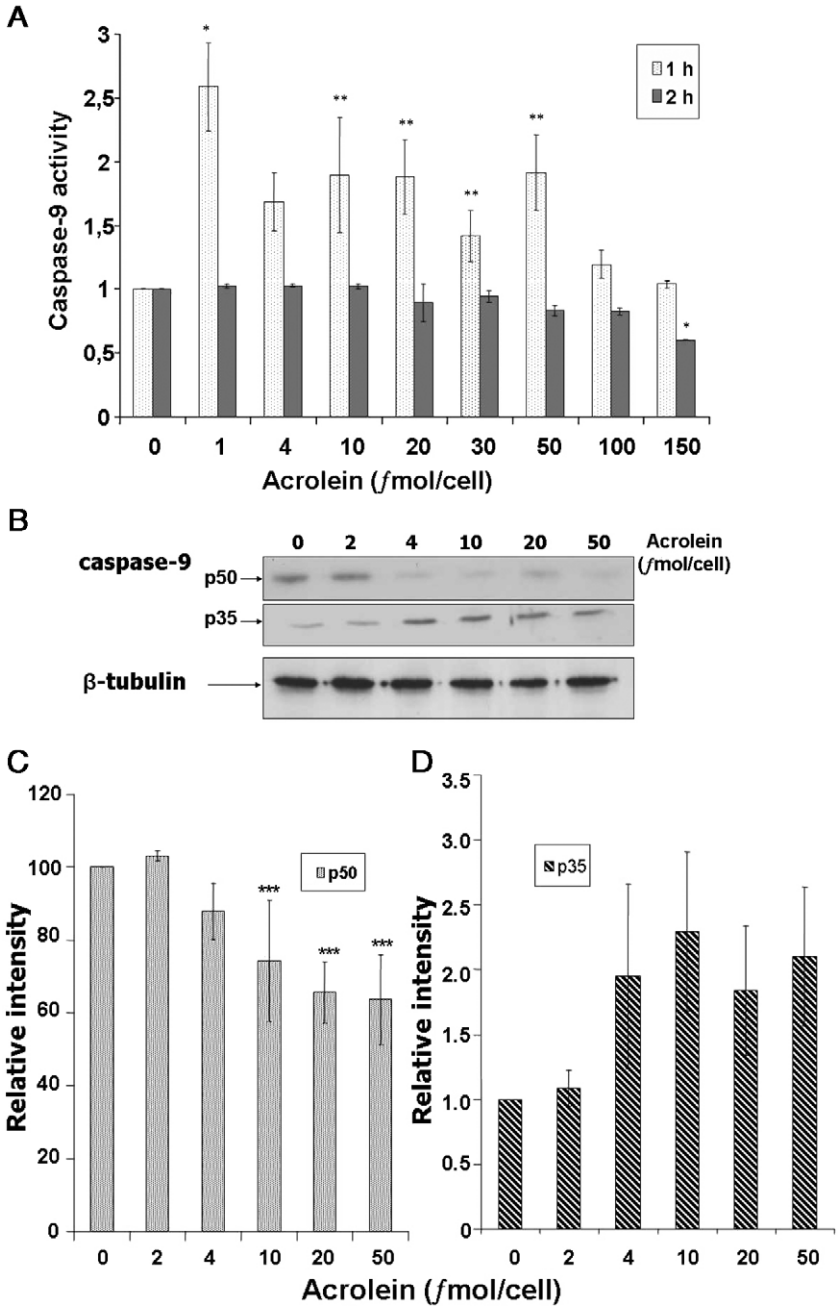

Fig. 4. Activation of initiator caspase-9 and cleavage of procaspase-9 by acrolein. (A) CHO cells (0.5×10^6/ml) were incubated with acrolein (1 to 150 fmol/cell) for 1 or 2 h in α-MEM with 10% FBS. Caspase-9 activity was measured in cell lysates using the fluorescent substrate Ac-LEHD-AFC. Caspase-9 activity was expressed relative to the untreated control, designated as 1. Data represent means and S.E. from eight independent experiments performed with multiple estimations per point. $P<0.05$ (*) or $P<0.01$ (**) indicates a statistically significant difference between acrolein treatment and the control. (B) Cells (10^6/ml) were incubated with acrolein (2 to 50 fmol/cell) for 1 h in α-MEM containing 10% FBS. The immunodetection of procaspase-9 and its cleavage fragment (35 kDa) was carried out by SDS-PAGE, using β-tubulin as a loading control. A representative gel is shown from four independent experiments. Densitometric analyses of the expression of (C) procaspase-9 and (D) the cleavage fragment are relative to the untreated control. $P<0.001$ (***) indicates a statistically significant difference between treatment with acrolein and the control.

completely inhibited caspase-3 activity (Fig. 5A). Although caspase-3 activity was inhibited, procaspase-3 was cleaved (Fig. 5B, C) to its two fragments p11 and p17 (Fig. 5B, D). The cleavage of pro-caspase-3 is necessary for the formation of the active dimeric form of caspase-3 [41].

Since the effector caspase-3 was not activated, we determined whether other downstream caspases could be activated, in order to explain the acrolein-induced chromatin condensation (Fig. 2C). We evaluated the effect of acrolein on the activity of caspase-7, which is a downstream caspase that can cleave PARP. Thus, 10

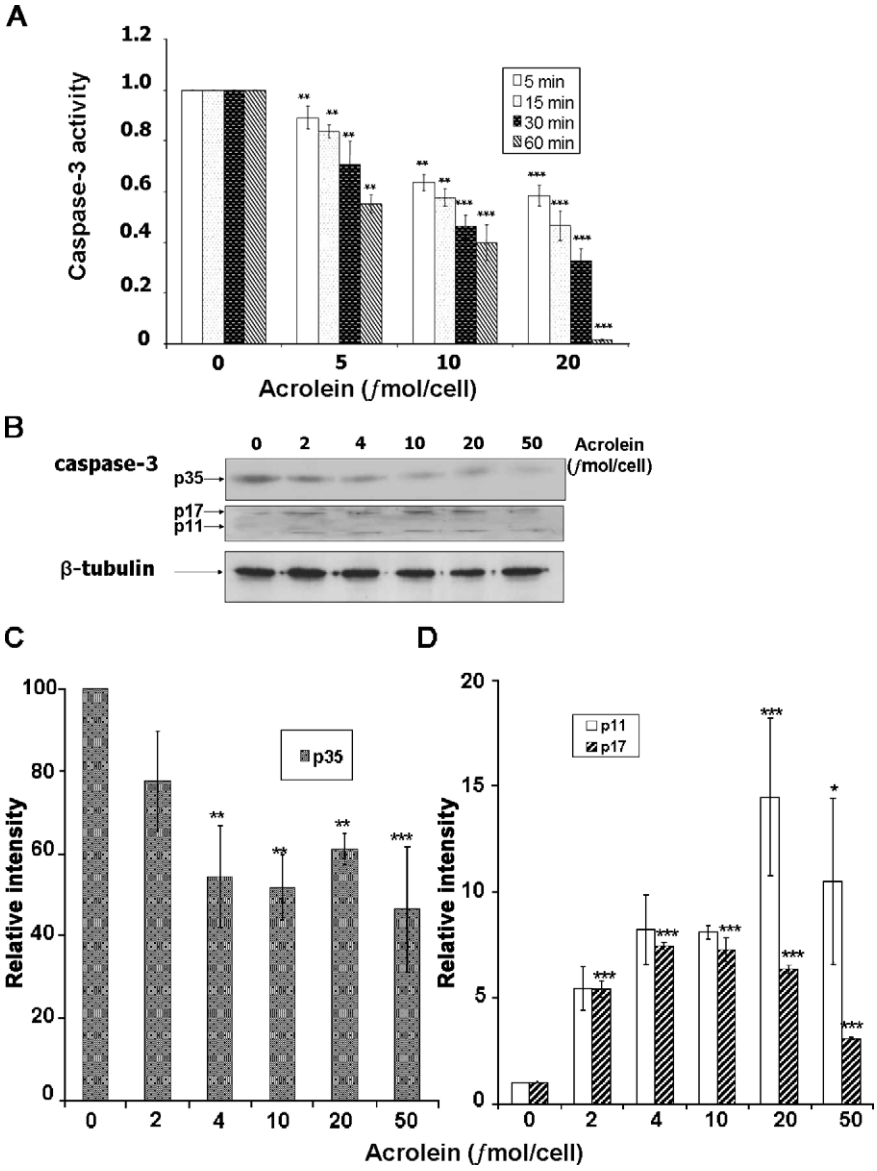

Fig. 5. Acrolein cleaves procaspase-3 but inhibits the enzymatic activity of caspase-3. (A) CHO cells (0.5×10^6/ml) were incubated with acrolein (5 to 20 fmol/cell) for 5, 15, 30, and 60 min in α-MEM containing 10% FBS. Caspase-3 activity was measured in cell lysates using the fluorescent substrate Ac-DEVD-AMC. Caspase-3 activity was expressed relative to the untreated control, designated as 1. Data represent means and S.E. from seven independent experiments performed with multiple estimations per point. $P<0.01$ (**) or $P<0.001$ (***) indicates a statistically significant difference between acrolein treatment and the control. (B) Cells (10^6/ml) were incubated with acrolein (2 to 50 fmol/cell) for 1 h in α-MEM containing 10% FBS. The immunodetection of procaspase-3 and its cleavage fragments (11 and 17 kDa) was carried out by SDS-PAGE, using β-tubulin as a loading control. A representative gel is shown from four independent experiments. Densitometric analyses of the expression of (C) procaspase-3 and (D) the cleavage fragments are relative to the untreated control. $P<0.05$ (*), $P<0.005$ (**), or $P<0.001$ (***) indicates a statistically significant difference between treatment with acrolein and the control.

fmol/cell of acrolein, which inhibited caspase-3 after 5 min of exposure (Fig. 5A), activated caspase-7 after 2 h (Fig. 6A). Similar to caspase-3, the cleavage of procaspase-7 is necessary for the formation of the active dimeric form of caspase-7 [41]. Indeed, the cleavage of procaspase-7 (Fig. 6B, C) to its active fragment p20 (Fig. 6B, D) was induced after 1 h, by 10 to 50 fmol/cell of acrolein. Higher concentrations of acrolein (≥100 fmol/cell) were needed to activate caspase-7 after 1 h, whereas lower concentrations (10 and 50 fmol/cell) activated the enzyme after 2 h of acrolein exposure (Fig. 6A). Higher doses of acrolein (>100 fmol/cell) did not activate caspase-7 after 2 h (Fig. 6A).

The subsequent step was to confirm the implication of caspase-9 in acrolein-induced apoptosis. Therefore, the ability of a general inhibitor of caspases and of specific inhibitors of caspases-3 and -9 to inhibit apoptosis induced by acrolein was evaluated. The level of apoptosis was partially inhibited by the general inhibitor of caspases (Fig. 7A). The inhibitor of caspase-9 decreased

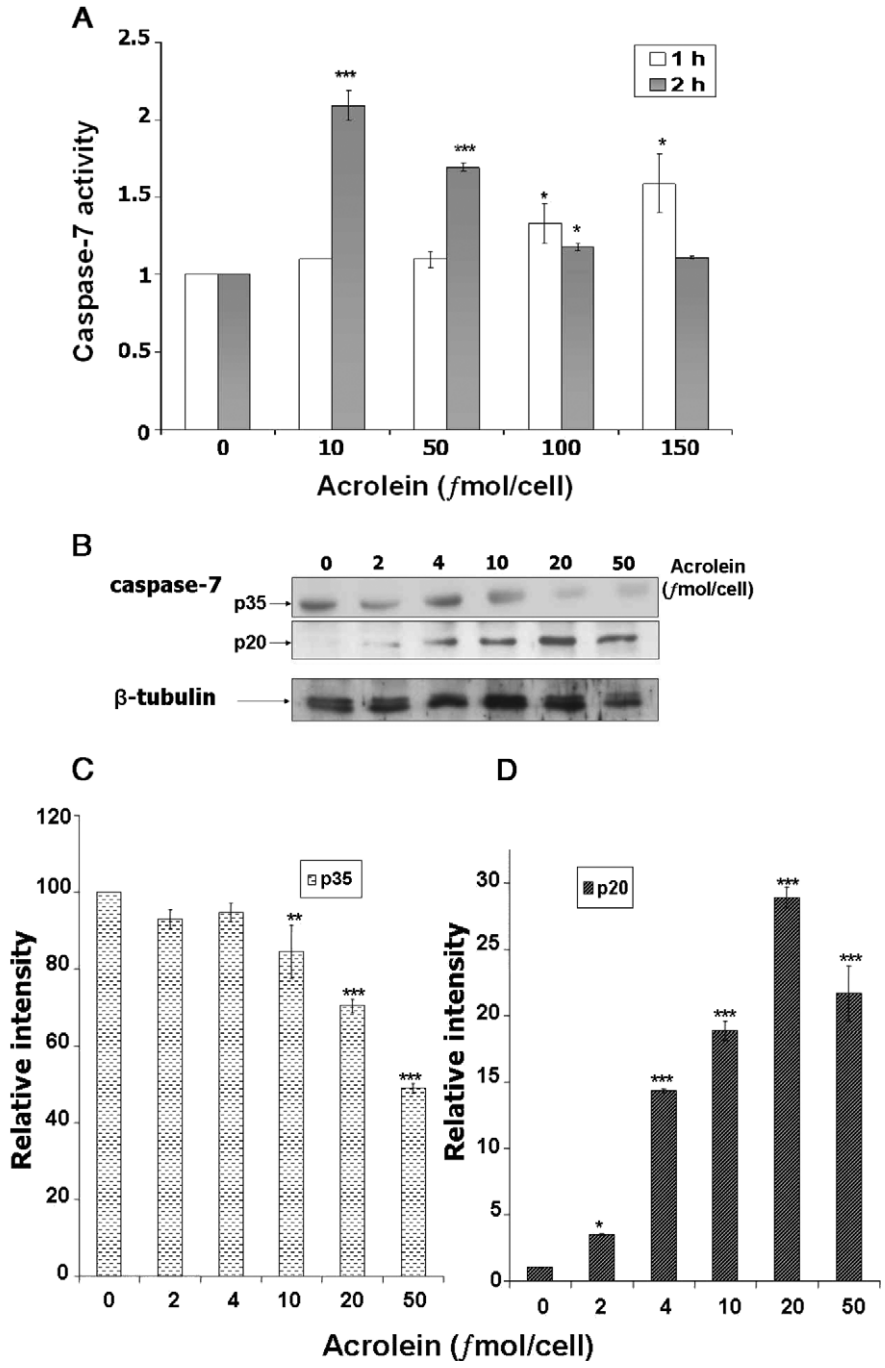

Fig. 6. Acrolein activates caspase-7 and cleaves procaspase-7. (A) CHO cells (0.5×10^6/ml) were incubated with acrolein (10 to 150 fmol/cell) for 1 and 2 h in α-MEM containing 10% FBS. Caspase-7 activity was measured in cell lysates using the fluorescent substrate MCA-VDQVDGWK-(DNP)-NH2. Caspase-7 activity was expressed relative to the untreated control, designated as 1. Data represent means and S.E. from seven independent experiments performed with multiple estimations per point. $P< 0.05$ (*) or $P< 0.001$ (***) indicates a statistically significant difference between acrolein treatment and the control. (B) Cells (10^6/ml) were incubated with acrolein (2 to 50 fmol/cell) for 1 h in α-MEM containing 10% FBS. The immunodetection of procaspase-7 and its cleavage fragment (20 kDa) was carried out by SDS-PAGE, using β-tubulin as a loading control. A representative gel is shown from four independent experiments. Densitometric analyses of the expression of (C) procaspase-7 and (D) the cleavage fragment are relative to the untreated control. $P<0.05$ (*), $P<0.005$ (**), or $P<0.001$ (***) indicates a statistically significant difference between treatment with acrolein and the control.

cell death by apoptosis by about 70% (Fig. 7A). However, the inhibitor of caspase-3 had no effect on apoptosis induced by acrolein (Fig. 7B). Hydrogen peroxide was used as a positive control to show that the inhibitor of caspase-3 was able to inhibit peroxide-induced apoptosis (Fig. 7C).

Acrolein (≥50 fmol/cell) induced cleavage of the caspase substrate ICAD, the inhibitor of caspase acti-

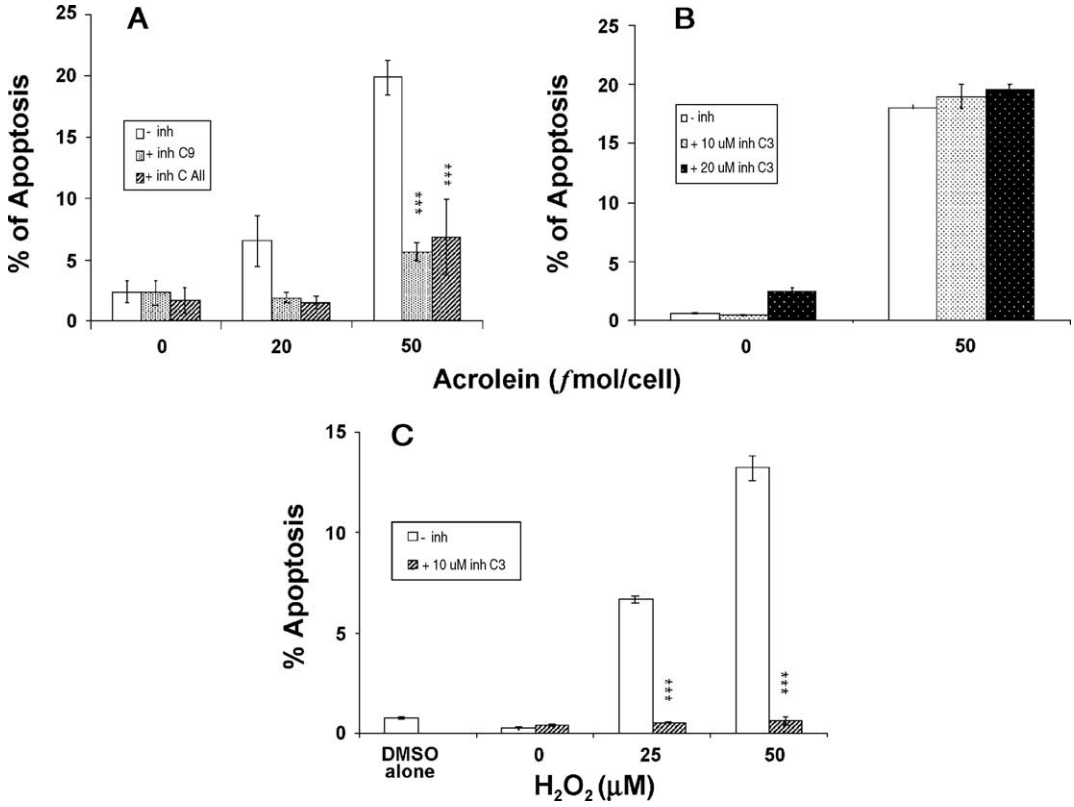

Fig. 7. Inhibition of apoptosis induced by acrolein by a specific inhibitor of caspase-9. Treatment with (A) 10 μM of caspase-9 inhibitor I, Z-LEHD-FMK, and 10 μM of general caspase inhibitor I, Z-VAD-FMK, (B) 10 or 20 μM of caspase-3 inhibitor V, Z-DQMD-FMK, and (C) 10 μM of caspase-3 inhibitor V, Z-DQMD-FMK (Calbiochem, La Jolla, CA), was performed on confluent cells in the monolayer. Cells were incubated with (A, B) acrolein (20 and 50 fmol/cell) or (C) H_2O_2 (25 and 50 μM) for 4 h with inhibitors present. The fraction of apoptotic cells (Hoechst) is given relative to total cells. A minimum of 600 cells was counted per dish. Data represent means and S.E. from five independent experiments performed with multiple estimations per point. (A, C) $P< 0.001$ (***) indicates a statistically significant difference between cells exposed to acrolein with and without caspase inhibitors.

vated DNase (CAD), after 2 h (Fig. 8), thereby liberating CAD, which can cause DNA fragmentation in the nucleus.

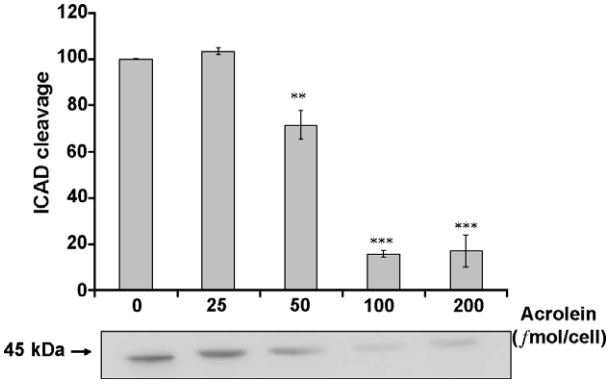

Fig. 8. Acrolein causes cleavage of ICAD. CHO cells (10^6/ml) were incubated with acrolein (25 to 200 fmol/cell) for 2 h in α-MEM containing 10% FBS. The immunodetection of ICAD was carried out using SDS-PAGE. The expression of ICAD was relative to the untreated control, designated as 100%. Data represent means and S.E. from four independent experiments performed with multiple estimations per point. $P<0.01$ (**) or $P<0.001$(***) indicates a statistically significant difference between acrolein treatment and the control.

4. Discussion

The new finding of the present study is that acrolein is capable of inducing the mitochondrial pathway of apoptosis involving the liberation of cytochrome *c* and the activation of certain caspases in proliferating cells. We provide new information on the molecular mechanisms by which acrolein induces apoptosis. The induction of apoptosis by acrolein was confirmed morphologically by the condensation of nuclear chromatin after 4 h, a later event in the apoptotic cascade, as well as by several earlier, upstream events associated with apoptosis at the mitochondrial and post-mitochondrial levels. At the mitochondrial level, acrolein caused a decrease in membrane potential, followed by the liberation of cytochrome *c* into the cytosol, after 1 h. At the post-mitochondrial level, cytochrome *c* is an essential component of the cytosolic apoptosome complex, along with Apaf1 and pro-caspase-9. Acrolein indeed induced the activation of initiator caspase-9 after 1 h and the effector caspase-7 after 1 to 2 h. Caspase activation was followed by the cleavage of ICAD after 2 h. This leads to the liberation of the protease CAD, which can cause later events such as chromatin condensation and fragmentation of DNA in the nucleus.

The activation of these caspases was confirmed by the cleavage of their pro-enzyme forms and the generation of appropriate cleavage fragments, as well as by the increase in their enzymatic activities. The role of caspase-9 was also confirmed using a specific caspase-9 inhibitor. At present, there is no specific inhibitor of caspase-7 available commercially.

The implication of the PTP and cytochrome *c* release in acrolein-induced apoptosis was assessed using cyclosporine A. Although the mechanisms of cytochrome *c* release are not completely understood, it is considered that cytochrome *c* can be released from the mitochondria via the PTP, as well as by the formation of channels on the membrane involving Bax [42]. The inhibition of apoptosis by cyclosporine A supports a role for PTP opening and release of cytochrome *c* in acrolein-induced apoptosis. The partial inhibition by cyclosporine A suggests that acrolein could also induce apoptosis by alternative mechanisms to the mitochondrial pathway and/or that cytochrome *c* can be released by several different mechanisms.

Our findings show that caspase-3 is not essential for the execution phase of acrolein-induced apoptosis in proliferating cells. This was demonstrated by the lack of activation of its enzymatic activity and the lack of inhibition of nuclear chromatin condensation by a specific inhibitor of caspase-3. It was reported that MCF-7 cells, which lack caspase-3, can still undergo apoptosis [41]. Indeed, acrolein-induced apoptosis in CHO cells appears to be mediated through the activation of the effector caspase-7. In addition to caspase-3, caspase-9 is able to directly cleave pro-caspase-7, leading to subsequent activation of caspase-7 [43]. In our study, the cleavage of ICAD is likely to be mediated by caspase-7 [44]. It is often difficult to distinguish between the involvement of caspase-3 and -7 in apoptosis since they share similar protein (PARP, ICAD) [19] and peptide (Ac-DEVD-AMC) substrates [45].

A surprising finding in our study was that pro-caspase-3 was indeed cleaved in the cells, yet the enzymatic activity of caspase-3 was markedly inhibited by acrolein. The cleavage of pro-caspase-3 is likely to result from the proteolytic action of the active caspase-9 [46]. Even though pro-caspase-3 undergoes cleavage to generate caspase-3 in cells, enzymatic activity appears to be immediately inhibited. This could arise through the direct alkylation of its active site cysteine residue by acrolein. The inhibition of caspase-3 by acrolein is in agreement with other studies. The inhibition of caspase-3 activity occurred in neutrophils after 2 to 8 h of treatment with 10 μM acrolein [23]. The activities of caspases-3, -8, and -9 were inhibited 12 h following a 30-min exposure to acrolein (5 to 40 μM) in murine proB lymphocytes [24]. For each of the caspases-3, -7, and -9, cleavage of the pro-enzyme form into cleavage fragments occurred in CHO cells. However, all of the caspase enzymes contain a nucleophilic active-site cysteine residue, and potentially they could all be inhibited by acrolein [23,47]. Acrolein appears to be causing some activation of caspases-7 and -9, while at the same time inhibiting their activity. It appears that caspases-7 and -9 are not resistant to inactivation by acrolein, but rather, they may be less susceptible to inactivation than caspase-3 is. Although acrolein appears to eventually inhibit enzymatic activity of each of these 3 caspases, caspases-9 and -7 were sufficiently activated to trigger caspase-dependent downstream events such as ICAD cleavage and chromatin condensation. The fact that acrolein completely inhibits caspase-3, whereas caspases-7 and -9 undergo some level of activation in CHO cells, could also be explained by the more restricted access of acrolein to the active site cysteine residues of caspases-7 and -9. It was reported that the major structural differences among the caspases occur at the active sites, whereas the rest of the structures are very similar. These structural differences at the active sites could affect access to the active site, as well as interactions with other molecules and could explain the differences in the substrate specificities among the different caspases [41].

It has recently been reported that proteolytic cleavage is neither required nor sufficient for the activation of monomeric initiator caspases such as caspase-9 [48]. Dimerization, rather than cleavage, appears to be the most important step for caspase-9 activation and formation of an active site. However, cleavage of the prodomain stabilizes the active form of caspase-9. There are several similarities between the activation of caspases-7 and -9. Interestingly, the caspase-9 dimer only contains one active site. The catalytic apparatus in the other domain is disabled due to steric clashes. This inactive domain is almost identical to that of the zymogen form of caspase-7, indicating that some structural similarities exist between caspases-7 and -9. Also, identical conformational changes leading to the formation of the active sites was reported for caspases-7 and -9, even though they are activated by different mechanisms: proteolysis versus dimerisation, respectively [48]. However, interdomain cleavage by initiator caspases is needed for the activation of executioners such as caspases-3 and -7 [48].

In general, different studies have reported variable findings in that acrolein can either cause or inhibit apoptosis, or cause predominantly necrosis rather than apoptosis. For example, acrolein (25 μM) caused apoptosis in isolated human alveolar macrophages, detected by morphological changes and DNA fragmentation, after 24 h [20]. Exposure to 50 μM acrolein for 24 h induced atypical apoptosis in primary cultures of human keratinocytes [21]. Acrolein stimulated apoptosis in the human lung epithelial cell line HBE1, as indicated by the externalisation of phosphatidylserine and DNA fragmentation, 24 h after a 30-min exposure to 10 to 25 μM acrolein [22]. In human neutrophils, however, acrolein (25 μM) inhibited the constitutive pathway of apoptosis [23]. In proB lymphoid cells, the cell death pathway was predominantly oncosis/necrosis, with only

low levels of apoptosis occurring at lower doses (<10 μM) [24]. These variable results could be due to the differences in biochemical factors determining cell death pathways in different cell types, which include non-proliferating primary cell cultures and cells involved in immune responses, as well as proliferating cancer cell lines. Furthermore, different methodologies were used in these studies, such as longer exposures to acrolein for 24 h or 48 h versus shorter exposures to acrolein for 30 to 60 min, with or without a 24-h recovery period. In some cases, including the present work, cells were exposed to acrolein in a medium containing serum [20], whereas other studies exposed cells in serum-free medium [21–24]. Acrolein can bind to serum proteins, which would likely decrease the concentration available to interact with cells. This may slow or modify the onset of toxicity, leading to apoptosis, rather than necrosis. Necrosis appeared to be the predominant form of cell death when cells were exposed to acrolein in a serum-free medium [24]. In our study, acrolein did induce necrosis, but at higher doses than those which caused apoptosis.

One of our interests in exploring mechanisms of acrolein toxicity in proliferating cells lies in the context of anticancer treatment. We reported that acrolein and H_2O_2 both contributed to the cytotoxicity induced by spermine and bovine serum amine oxidase (BSAO, EC 1.4.3.6) in CHO cells [49]. Since tumor tissues contain elevated levels of polyamines, targeting polyamines could be a promising therapeutic strategy [28]. Toxic products such as H_2O_2 and acrolein could be generated in situ by amine oxidases for the selective killing of tumor cells [49]. Furthermore, the enzyme could also act by depleting polyamines which are necessary for tumor growth. BSAO has been successfully immobilized in biocompatible polyethylene glycol hydrogels, which could be useful for in vivo stability and delivery of the enzyme to tumors [50].

In conclusion, this study clearly demonstrates that acrolein can cause cell death by both apoptosis and necrosis. A small elevation in acrolein concentration switched the mechanism of cell death from apoptosis to necrosis. Acrolein induced apoptosis through the mitochondrial pathway, involving cytochrome *c* release from the mitochondria and the activation of caspases. However, this does not rule out the possibility that acrolein could induce apoptosis by alternative or complementary mechanisms. Apoptosis could also occur via death receptor pathways without the involvement of cytochrome *c*. Furthermore, a cross-talk pathway exists between the death receptor and mitochondrial pathways, which also leads to cytochrome *c* release. Future studies will investigate the role of death receptor and cross-talk pathways in acrolein-induced apoptosis. The present findings may be important in explaining the pharmacological action and/or toxic side effects of cyclophosphamide, which has acrolein as one of its metabolites, as well as the toxicity of environmental exposures to low doses of acrolein in proliferating cells.

Acknowledgements

Financial support was obtained from the Natural Sciences and Engineering Research Council of Canada (DAB). The authors thank Stéphanie Lord-Fontaine and Michel Marion for technical assistance, and Bertrand Fournier (SCAD) for statistical analysis.

References

[1] J.P. Kehrer, S.S. Biswal, The molecular effects of acrolein, Toxicol. Sci. 57 (2000) 6–15.
[2] K. Uchida, Current status of acrolein as a lipid peroxidation product, Trends Cardiovasc. Med. 9 (1999) 109–113.
[3] M.T. Borchers, S. Wesselkamper, S.E. Wert, S.D. Shapiro, G.D. Leikauf, Monocyte inflammation augments acrolein-induced Muc5ac expression in mouse lung, Am. J. Physiol. 277 (1999) L489–L497.
[4] D.P. Ghilarducci, R.S. Tjeerdema, Fate and effects of acrolein, Rev. Environ. Contam. Toxicol. 144 (1995) 95–146.
[5] S. Biswal, G. Acquaah-Mensah, K. Datta, X. Wu, J.P. Kehrer, Inhibition of cell proliferation and AP-1 activity by acrolein in human A549 lung adenocarcinoma cells due to thiol imbalance and covalent modifications, Chem. Res. Toxicol. 15 (2002) 180–186.
[6] A. Furuhata, M. Nakamura, T. Osawa, K. Uchida, Thiolation of protein-bound carcinogenic aldehyde, an electrophilic acrolein-lysine adduct that covalently binds to thiols, J. Biol. Chem. 277 (2002) 27919–27926.
[7] D. Suzuki, T. Miyata, Carbonyl stress in the pathogenesis of diabetic nephropathy, Intern. Med. 38 (1999) 309–314.
[8] M.A. Lovell, C. Xie, W.R. Markesbery, Acrolein is increased in Alzheimer's disease brain and is toxic to primary hippocampal cultures, Neurobiol. Aging 22 (2001) 187–194.
[9] N.Y. Calingasan, K. Uchida, G.E. Gibson, Protein-bound acrolein: a novel marker of oxidative stress in Alzheimer's disease, J. Neurochem. 72 (1999) 751–756.
[10] K. Uchida, M. Kanematsu, Y. Morimitsu, T. Osawa, N. Noguchi, E. Niki, Acrolein is a product of lipid peroxidation reaction. Formation of free acrolein and its conjugate with lysine residues in oxidized low density lipoproteins, J. Biol. Chem. 273 (1998) 16058–16066.
[11] A. Saraste, K. Pulkki, Morphologic and biochemical hallmarks of apoptosis, Cardiol. Res. 45 (2000) 528–537.
[12] A.J. Hale, S.C.A. Mith, L.C. Sutherland, V.E. Stoneman, V. Longthorne, Apoptosis: molecular regulation of cell death, Eur. J. Biochem. 236 (1996) 1–26.
[13] C.B. Thompson, Apoptosis in the pathogenesis and treatment of disease, Science 267 (1995) 1456–1462.
[14] G.S. Salvesen, V.M. Dixit, Caspases: intracellular signaling by proteolysis, Cell 91 (1997) 443–446.
[15] G. Denecker, D. Vercammen, W. Declercq, P. Vandenabeele, Apoptotic and necrotic cell death induced by death domain receptors, Cell. Mol. Life Sci. 58 (2001) 356–370.
[16] S.E. Wilson, Stimulus-specific and cell type-specific cascades: emerging principles relating to control of apoptosis in the eye, Exp. Eye Res. 69 (1999) 255–266.
[17] J. Chandra, A. Samali, S. Orrenius, Triggering and modulation of apoptosis by oxidative stress, Free Radic. Biol. Med. 29 (2000) 323–333.
[18] A. Kelekar, C.B. Thompson, Bcl-2 family proteins: the role of the BH3 domain in apoptosis, Trends Cell Biol. 8 (1998) 324–330.
[19] M. Germain, E.B. Affar, D. D'Amours, V.M. Dixit, G.S. Salvesen, G.G. Poirier, Cleavage of automodified poly(ADP-ribose) polymerase during apoptosis. Evidence for involvement of caspase-7, J. Biol. Chem. 274 (1999) 28379–28384.

[20] L. Li, R.F. Hamilton, D.E. Taylor, A. Holian, Acrolein-induced cell death in human alveolar macrophages, Toxicol. Appl. Pharmacol. 145 (1997) 331–339.
[21] K. Takeuchi, M. Kato, H. Suzuki, A.A. Akhand, J. Wu, K. Hossain, T. Miyata, Y. Matsumoto, Y. Nimura, I. Nakashima, Acrolein induces activation of the epidermal growth factor receptor of human keratinocytes for cell death, J. Cell. Biochem. 81 (2001) 679–688.
[22] M. Nardini, E.I. Finkelstein, S. Reddy, G. Valacchi, M. Traber, C.E. Cross, A. van der Vliet, Acrolein-induced cytotoxicity in cultured human bronchial epithelial cells, Modulation by alpha-tocopherol and ascorbic acid, Toxicology 170 (2002) 173–185.
[23] E.I. Finkelstein, M. Nardini, A. van der Vliet, Inhibition of neutrophil apoptosis by acrolein: a mechanism of tobacco-related lung disease? Am. J. Physiol., Lung Cell. Mol. Physiol. 281 (2001) L732–L739.
[24] J.C. Kern, J.P. Kehrer, Acrolein-induced cell death: a caspase-influenced decision between apoptosis and oncosis/necrosis, Chem.-Biol. Interact. 1 (2002) 79–95.
[25] P.S. Schwartz, D.J. Waxman, Cyclophosphamide induces caspase 9-dependent apoptosis in 9 L tumor cells, Mol. Pharmacol. 60 (2001) 1268–1279.
[26] E. Agostinelli, E. Przybytkowski, D.A. Averill-Bates, Glucose, glutathione, and cellular response to spermine oxidation products, Free Radic. Biol. Med. 5 (1996) 649–656.
[27] S. Lord-Fontaine, E. Agostinelli, E. Przybytkowski, D.A. Averill-Bates, Amine oxidase, spermine, and hyperthermia induce cytotoxicity in *P*-glycoprotein overexpressing multidrug resistant Chinese hamster ovary cells, Biochem. Cell. Biol. 79 (2001) 165–175.
[28] O. Heby, L. Persson, Molecular genetics of polyamine synthesis in eukaryotic cells, Trends Biochem. Sci. 15 (1990) 153–158.
[29] U. Bachrach, Y.M. Heimer, The physiology of polyamines, CRC Press, Boca Raton, FL, 1989.
[30] D.A. Averill-Bates, E. Agostinelli, E. Przybytkowski, M.A. Mateescu, B. Mondovi, Cytotoxicity and kinetic analysis of purified bovine serum amine oxidase in the presence of spermine in Chinese hamster ovary cells, Arch. Biochem. Biophys. 300 (1993) 75–79.
[31] V. Ling, L.H. Thompson, Reduced permeability in CHO cells as a mechanism of resistance to colchicines, J. Cell. Physiol. 83 (1974) 103–116.
[32] D.A. Bates, W.J. Mackillop, Hyperthermia, adriamycin transport, and cytotoxicity in drug-sensitive and -resistant Chinese hamster ovary cells, Cancer Res. 46 (1986) 5477–5481.
[33] Y.J. Lee, E. Shacter, Oxidative stress inhibits apoptosis in human lymphoma cells, J. Biol. Chem. 274 (1999) 19792–19798.
[34] H.R. Stennicke, G.S. Salvesen, Biochemical characteristics of caspases-3, -6, -7, and -8, J. Biol. Chem. 272 (1997) 25719–25723.
[35] Z. Darzynkiewicz, S. Bruno, G. Del Bino, Features of apoptotic cells measured by flow cytometry, Cytometry 13 (1992) 795–808.
[36] U.K. Laemmli, Cleavage of structural proteins during the assembly of the head of bacteriophage T4, Nature 227 (1970) 680–885.
[37] M.M. Bradford, A rapid and sensitive method for the quantitation of microgram quantities of protein utilizing the principle of protein-dye binding, Anal. Biochem. 72 (1976) 248–254.
[38] P.H. Westfall, R.D. Tobias, D. Rom, D. Russel, Y. Hochberg (Eds.), Multiple Comparisons and Multiple Tests Using the SAS System, SAS Publishing, Cary, NC, 1999.
[39] N.D. Horton, B.M. Mamiya, J.P. Kehrer, Relationships between cell density, glutathione, and proliferation of A549 human lung adenocarcinoma cells treated with acrolein, Toxicology 122 (1997) 111–122.
[40] J. Henry-Mowatt, C. Dive, J.C. Martinou, D. James, Role of mitochondrial membrane permeabilization in apoptosis and cancer, Oncogene 23 (2004) 2850–2860.
[41] A. Degterev, M. Boyce, J. Yuan, A decade of caspases, Oncogene 22 (2003) 8543–8567.
[42] S. Orrenius, B. Zhivotovsky, P. Nicotera, Regulation of cell death: the calcium–apoptosis link, Nat. Rev., Mol. Cell Biol. 4 (2003) 552–565.
[43] E.A. Slee, M.T. Harte, R.M. Kluck, B.B. Wolf, C.A. Casiano, D.D. Newmeyer, H.G. Wang, J.C. Reed, D.W. Nicholson, E.S. Alnemri, D.R. Green, S.J. Martin, Ordering the cytochrome *c*-initiated caspase cascade: hierarchical activation of caspases-2, -3, -6, -7, -8, and -10 in a caspase-9-dependent manner, J. Cell Biol. 144 (1999) 218–292.
[44] B.B. Wolf, M. Schuler, F. Echeverri, D.R. Green, Caspase-3 is the primary activator of apoptotic DNA fragmentation via DNA fragmentation factor-45/inhibitor of caspase-activated DNase inactivation, J. Biol. Chem. 274 (1999) 30651–30656.
[45] G.M. Cohen, Caspases: the executioners of apoptosis, Biochem. J. 326 (1997) 1–16.
[46] A. Lawen, Apoptosis—an introduction, Bioessays 9 (2003) 888–896.
[47] J.B. Mannick, A. Hausladen, L. Liu, D.T. Hess, M. Zeng, Q.X. Miao, L.S. Kane, A.J. Gow, J.S. Stamler, Fas-induced caspase denitrosylation, Science 284 (1999) 651–654.
[48] K.M. Boatright, G.S. Salvesen, Mechanisms of caspase activation, Curr. Opin. Cell Biol. 15 (2003) 725–731.
[49] D.A. Averill-Bates, E. Agostinelli, E. Przybytkowski, B. Mondovi, Aldehyde dehydrogenase and cytotoxicity of purified bovine serum amine oxidase and spermine in Chinese hamster ovary cell, Biochem. Cell. Biol. 72 (1994) 36–42.
[50] N. Demers, E. Agostinelli, D.A. Averill-Bates, G. Fortier, Immobilization of native and poly(ethylene glycol)-treated ('PEGylated') bovine serum amine oxidase into a biocompatible hydrogel, Biotechnol. Appl. Biochem. 3 (2001) 201–207.